2024-01

# Production and preservation of organic carbon in sub-seafloor tephra layers

Longman, J



10.1016/j.marchem.2023.104334
Marine Chemistry
Elsevier

Marine Chemistry 258 (2024) 104334

Contents lists available at ScienceDirect

Marine Chemistry

journal homepage: www.elsevier.com/locate/marchem

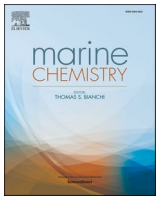

# Production and preservation of organic carbon in sub-seafloor tephra layers

Jack Longman [a,b,c,1,*], Hayley R. Manners [b,d,1], Thomas M. Gernon [b], James McManus [e], Martin R. Palmer [b], Steven J. Rowland [d], Paul A. Sutton [d]

[a] Marine Isotope Geochemistry, Institute for Chemistry and Biology of the Marine Environment (ICBM), University of Oldenburg, Oldenburg, Germany
[b] School of Ocean and Earth Sciences, University of Southampton, Southampton, UK
[c] Department of Geography and Environmental Sciences, Northumbria University, Newcastle-Upon-Tyne, UK
[d] School of Geography, Earth and Environmental Sciences, University of Plymouth, Plymouth, UK
[e] Bigelow Laboratory for Ocean Sciences, East Boothbay, ME, USA

ARTICLE INFO

*Keywords:*
Tephra
Organic carbon
Microbial carbon
Marine sediment
Autotrophy

ABSTRACT

The deposition of volcanic ash into the ocean initiates a range of chemical and biological reactions. During diagenesis, these reactions may enhance the preservation of organic carbon (OC) in marine sediments, which ultimately promotes $CO_2$ sequestration from the ocean-atmosphere system. However, this interpretation is reliant on a small number of studies that make a link between tephra and OC burial. Here, we compare organic and inorganic geochemical data from tephra-bearing marine sediments from three sites that differ widely in their location, age, and composition. We show that OC is buried in, and proximal to, tephra layers, in proportions higher than would be expected via simple admixture of surrounding sediment. Our data indicate that this OC is preserved primarily through interactions with reactive iron phases, which act to physically protect the carbon from oxidation. Analysis of the composition of the OC associated with reactive iron indicates it is isotopically (consistently more negative $\delta^{13}C$ than sediment) and chemically (comprised of compounds not found in the sediment) distinct from OC in the background sediments. We interpret this signal as indicating a microbial source of OC, with autochthonous OC production resulting from autotrophic microbial exploitation of nutrients supplied from tephra. This finding has implications for our understanding of carbon cycling on Earth, and possibly for the emergence of life in terrestrial and perhaps even extra-terrestrial environments.

## 1. Introduction

Addition of volcanic ash to marine sediments enhances organic carbon (OC) burial rates via a variety of mechanisms (Longman et al., 2019). The input of fresh tephra to the oceans may stimulate primary productivity (Langmann et al., 2010; Olgun et al., 2011), enhancing the export of OC from the upper ocean via the ballasting effect of ash (Pabortsava et al., 2017). Once tephra reaches the seafloor, consumption of oxygen via the oxidation of reactive iron ($Fe_R$) phases may prevent microbial degradation of OC (Hembury et al., 2012; Straub and Schmincke, 1998). $Fe_R$ also provides physical protection for OC (Lalonde et al., 2012), inhibiting its breakdown and remineralisation (Longman et al., 2021b). In some environments, such as the Sea of Okhotsk and the Hikurangi Margin, tephra may also supply cations for authigenic carbonate formation (Luo et al., 2023; Luo et al., 2020; Torres et al., 2020; Wallmann et al., 2008), converting available OC into a form of carbon that is stable for millions of years (Longman et al., 2021a).

Evidence that combines records of ash deposition and climatic change suggests that during periods in Earth's history characterized by intense and sustained ashfall, such as the late Ordovician and Cretaceous Periods, enhanced OC burial led to considerable carbon drawdown and global cooling (Lee et al., 2018; Longman et al., 2021c). Further, it has been suggested that augmentation of the supply of tephra to the oceans could represent a viable greenhouse gas removal method today, leveraging the ability of tephra to enhance OC burial (Longman et al., 2020). However, our understanding of these processes is limited, with only a small number of studies systematically investigating the record of OC burial in tephra-containing marine sediments (Inagaki et al., 2003; Li et al., 2020, 2023; Longman et al., 2021b). In particular, the composition of OC preserved as a result of tephra deposition is largely unknown, though preliminary work suggests it is isotopically distinct from OC preserved in normal marine sediments (Longman et al., 2021b).

* Corresponding author at: Department of Geography and Environmental Sciences, Northumbria University, Newcastle-Upon-Tyne, UK.
*E-mail address:* jack2.longman@northumbria.ac.uk (J. Longman).
[1] These authors contributed equally

https://doi.org/10.1016/j.marchem.2023.104334
Received 11 August 2023; Received in revised form 1 November 2023; Accepted 16 November 2023
Available online 23 November 2023

One possibility for this isotopically distinct OC is that tephra deposition acts to support subseafloor microbial communities. Tephra deposition in the oceans can both stimulate and suppress the activity of sea-surface microbial, phytoplankton, and zooplankton communities (Browning et al., 2014; Wall-Palmer et al., 2011; Zhang et al., 2017). Similarly, once the tephra is deposited on the seafloor, differential responses of micro- and macro-benthic communities to the arrival of volcanic material have been recorded (Hess et al., 2001; Hess and Kuhnt, 1996; Li et al., 2020; Song et al., 2014). Genomic studies suggest that stimulation of autotrophic microbial activity in seafloor tephra layers likely arises because freshly deposited volcanic material contains reactive metals (particularly iron) that can act as an energy source of metal-related metabolic pathways (Li et al., 2020). While active seafloor biological communities influenced by tephra have been studied, the biomarkers of microbial activity in tephra layers have received less attention (Li et al., 2023). This lack of biomarker study is understandable because studies of biomarkers in older sediments are largely concerned with reconstructing paleo-environmental conditions, and tephra layers are largely viewed as an inert component useful only as datable horizons (cf. Lowe, 2011). However, this lack of research is potentially consequential because the large eruptive flux of tephra from subaerial explosive eruptions ($\sim 10^{12}$ kg $yr^{-1}$; Pyle, 1995) means that tephra is a near ubiquitous component of marine sediments (Lowe, 2011). In addition, both the redox state and presence of reactive Fe phases in subseafloor tephra enhance the preservation of organic carbon within tephra layers (Hembury et al., 2012; Homoky et al., 2011; Longman et al., 2019). Hence, tephra layers may contain a record of the presence of current and past episodes of microbial activity that may not be preserved in non-tephra bearing sediments.

Here, we report the results of a study of the organic carbon isolated from tephra layers collected from three marine volcanogenic-rich sedimentary environments, as well as background sediment compositions (biogenic siliceous ooze, hemipelagic calcareous and terrigenous mudrock). These sites, from offshore Montserrat, the Bering Sea, and the North Atlantic Ocean, span a range of ages from the Eocene to the present day. We apply a range of conventional geochemical tools to investigate the organic carbon associated with these layers. This approach allows us to rigorously investigate the types of OC preserved in tephra-rich sediments. By analysing sediments from a range of sites, and a range of tephra styles, we can identify differences in sedimentary diagenetic reactions relating to changes in these variables.

## 2. Materials and methods

### 2.1. Study sites

Sediments from Hole U1339D of IODP Expedition 323 (54°31.26′N, 169°44.35′W, 200 m below sea level (mbsl)), on the Umnak Plateau in the Bering Sea largely comprise two lithological endmembers: biogenic diatom-rich sediment and a volcanogenic component. The volcanogenic material is sourced from various volcanic eruptions along the Aleutian arc and constitutes ~4–40% of the sediment (Takahashi et al., 2011; Vaughn and Caissie, 2017). Sediments at Hole U1396C of IODP Expedition 340 (16°30.49′N, 62°27.10′W; 801 mbsl) are dominated by background biogenic carbonate punctuated by intermittent deposition of volcanic material derived largely from the volcanically active island of Montserrat (Le Friant et al., 2013). Samples were also taken from DSDP Holes 553 A and 555 in the Rockall Plateau of the northeast Atlantic (DSDP leg 81, 56°05.32′N; 23°20.61′W; 1659 mbsl, and 56°33.70′N; 20°46.93′W; 2329 mbsl, respectively). These cores consist dominantly of early-Eocene mud rocks with extensive tephra deposits (Backman et al., 1984; Roberts et al., 1984).

Sampling followed the same protocols at each site. After visual identification of cores, subsampling of both tephra layers and sediment was undertaken. The surface of the split-core sections was removed, and care was taken to ensure that only the centre of the tephra layers was sampled to avoid contamination from the adjacent sediments. For Hole U1339D, samples were selected around tephra layers in the uppermost 200 m of the core; the lowermost samples were approximately 750 kyr old (Takahashi et al., 2011). For Hole U1396C, samples were taken from the uppermost 140 m of the core, with the aim of sampling both tephra and sediment, with the oldest samples formed ca. 4 Myr ago (Palmer et al., 2016; Wall-Palmer et al., 2014). For Hole 553 A samples were selected from sections 36R1 to 36R3, between 483.5 and 487.7 mbsf. A range of samples from Hole 555 were analyzed; from 561 to 939 mbsf. For both Holes 553 A and 555, samples are of late Paleocene to early Eocene age (c. 60–50 Ma) (Backman et al., 1984).

### 2.2. Carbon concentrations

For Hole U1396C, 339 samples (164 sediments and 175 tephra) were analyzed for total carbon (TC), organic carbon (OC) and inorganic carbon (IC) contents. The tephra samples were prepared and analyzed at the University of Plymouth, where they were freeze dried and powdered prior to de-carbonation by treatment with excess hydrochloric acid (10%, *v*/v) until any visible sign of reaction had ceased. Samples were then freeze dried again and placed into an elemental analyser, where they were combusted in an inert atmosphere. A calibration standard (L-cysteine) and certified reference material (CRM: PACS-1 sediment) were used to monitor analytical precision (< 0.3% variability). Background sediment samples from Hole U1396C were analyzed at Oregon State University, with 20–30 mg of each sample weighed into silver boats and exposed to hydrochloric acid vapor to remove all inorganic carbon prior to combustion analysis (Goñi et al., 2003). Precision was estimated via triplicate analysis of a selection of samples, with precision between 0.002 and 0.01 wt%, and with all standard deviations <5% of mean value. Data are reported as weight percent carbon and $CaCO_3$ was calculated as the difference between TC and TOC.

For Hole U1339D, 379 samples (281 sediments and 98 tephra) were analyzed. For Hole 553 A and Hole 555, a total of 153 samples were analyzed (122 sediments and 31 tephra). For Holes U1339D, 553 A and 555, OC measurements were carried out on a Vario PYRO cube Element Analyser (EA) coupled to a vision isotope ratio mass spectrometer (IRMS) at the University of Southampton. Approximately 20 mg of homogenised sample was acidified in perchloric acid to remove any carbonate prior to multiple rinses with Milli-Q water. EA quality control was performed via repeated measurements of High Organic Sediment Standard (HOSS; Element Microanalysis Ltd.), and acetanilide, with a precision of ±0.07 wt% and ± 0.1 wt%, respectively. Inorganic carbon (IC) analysis was completed via coulometry of evolved $CO_2$ after perchloric acid addition. Calibration was performed using a pure carbonate standard (CAS #471–34-1), and quality control was completed via analysis of an in-house stream sediment standard at the University of Southampton.

### 2.3. Stable Carbon isotopes

Bulk sediment carbon isotope (IC + OC) signatures ($\delta^{13}C_{Bulk}$) were measured on $CO_2$ evolved from EA combustion for Holes U1339D, 553 A and 555, and calibrated to USGS 40 and USGS 41a, with a reproducibility of ±0.02 ‰, and ± 0.09 ‰, respectively. Repeat analyses of HOSS ($n$ = 11), and acetanilide ($n$ = 8) were used for quality control, with precisions of ±0.04 ‰ and ± 0.05 ‰, respectively.

### 2.4. Total organic extract analysis

Lipid extraction was conducted on 56 samples from U1396 (48 sediment, 8 tephra) and 18 from Hole 553 A (15 sediment and 3 tephra) using a modified Bligh and Dyer method (White et al., 1979), with both tephra and sediment samples treated in the same manner. Samples were first freeze dried and crushed using and agate pestle and mortar. Samples were extracted using dichloromethane/methanol/phosphate buffer

(DCM/MeOH/phosphate buffer; 5 × 3.8 mL; 1:2:0.8, *v*/v/v), after which the ratio of the DCM/MeOH/phosphate buffer mixture was modified (1:1:0.8, v/v/v), allowing collection of the organic phase. All extractions were completed in glassware combusted at 400 °C in an inert atmosphere (Pasteur pipettes and vials) to ensure no contamination, with method blanks also completed (see Supplementary Fig. 1 for an example of a blank GC/MS total ion chromatogram). To ensure no plastic contamination impacted our interpretation, we also extracted and analyzed plastic bags, scoops and core liners in the same manner as the samples, shown in GC/MS total ion chromatograms in Supplementary Fig. 2. The organic extract was washed with deionized water and dried with anhydrous sodium sulfate. Residual solvent was removed under a $N_2$ stream at 40 °C to obtain the total organic extract (TOE). TOEs were rested and re-weighed to obtain TOE masses. TOEs were then made up to 1 mg $mL^{-1}$ and a subsample taken and derivatised (BSTFA +1% TMCS; 99:1; 70 °C, 1 h, heater block) for analysis using high temperature gas chromatography – flame ionization detection (HTGC-FID) and gas chromatography – mass spectrometry (GC–MS; (Sutton and Rowland, 2012).

All trimethylsilylated TOEs were analyzed using HTGC-FID to screen samples prior to GC–MS analysis. HTGC-FID was conducted using an Agilent 6890 gas chromatograph fitted with an autosampler (0.5 μL injection into cool-on-column inlet in track oven mode, +3 °C), a Vf-5ht Ultimetal column (15 m × 0.25 mm × 0.10 μm; Agilent Technologies UK Ltd., Cheshire, UK) with helium carrier gas (constant flow mode, 1 mL $min^{-1}$), an FID at 435 °C and the GC oven programmed from 40 to 430 °C at 15 °C $min^{-1}$, 10 min hold. GC–MS was conducted using an Agilent 7890 A gas chromatograph coupled to an Agilent 5975C quadrupole triple axis mass spectrometer, operating in electron impact mode (EI; 70 eV) and scanning mass range *m/z* 50–900. The gas chromatograph was fitted with a HP-5MS capillary column (30 m × 0.25 mm × 0.25 μm; Agilent Technologies UK Ltd., Cheshire, UK) suitable for analysis of apolar samples. Samples were injected (1 μL) in splitless mode (300 °C) with helium carrier gas (constant flow, 1 mL $min^{-1}$) and the GC oven programmed from 40 to 300 °C at 10 °C $min^{-1}$ with a 10 min hold. The transfer line was maintained at 280 °C and the ion source at 230 °C. The *n*-ethyl-4-benzenesulphonamide was identified by comparison of mass spectra of unknowns with that of authentic *n*-ethyl-4-benzenesulphonamide (Sigma Aldrich 415,367) and was further identified using data in the NIST Mass Spectral Database (NIST 08 MS library and MS search program v2.0f) and by GC retention time comparisons.

### 2.5. Reactive oxide analysis

A total of 37 samples from Holes 553 A and 555 were analyzed for total reactive iron (FeR) content and compared with previously published data from Hole U1339D (Longman et al., 2021b). For this, we used the sodium dithionite extraction process of Kostka and Luther (1994) which, despite several potential drawbacks, including incomplete removal of all oxides (Fisher et al., 2020; Longman et al., 2022), is the most widely utilised approach. Briefly, 0.1 g of freeze-dried sediment was leached in 4 mL of a 0.35 M sodium acetate, 0.2 M sodium citrate solution. To this, 0.1 M sodium dithionite was added, before mixing and heating to 60 °C in a water bath. The tube was shaken every 5 min, and after 15 min, centrifuged, and the supernatant decanted. HCl (200 μL) was added to prevent Fe(III) precipitation. The remaining sediment was then rinsed with deionized water and then freeze-dried. The acidified supernatant was analyzed on a Thermo X-Series ICP-MS instrument at the University of Southampton. Alongside the samples, Chilean Margin sediment (RR9702A-42MC, see Roy et al., 2013) was extracted and analyzed. $Fe_R$ content of this standard was 10,300 ± 400 ppm, similar to previous measured values of 10,800 ± 800 ppm (Roy et al., 2013), 9300 ± 200 ppm (Murray et al., 2016) and 10,475 ± 125 (Longman et al., 2021b).

To investigate the composition of the carbon associated with the $Fe_R$ phases, the approach of Lalonde et al. (2012) was used. This analysis compares the OC content and $\delta^{13}C$ composition of the sediment before and after extraction, following the methods outlined in sections 2.2 and 2.3. The amount of OC lost during the extraction (hereafter fOC-$Fe_R$) is calculated using the following equation:

$$fOC - Fe_{R} = \frac{OC_{extract}}{OC_{bulk}}$$

Where $OC_{extract}$ is the OC content after extraction and $OC_{bulk}$ is the content before. The isotopic composition of the extracted OC is calculated using the following equation:

$$\delta^{13}C_{Fe-OC} = \frac{\delta^{13}C_{bulk} \times OC_{bulk} - \delta^{13}C_{Fe-OC-extract} \times OC_{extract}}{OC_{bulk} - OC_{extract}}$$

where $\delta^{13}C_{bulk}$ is the $\delta^{13}C$ of OC before the dithionite experiment and $\delta^{13}C_{Fe\text{-}OC\text{-}extract}$ is the $\delta^{13}C$ of OC after the dithionite extraction.

## 3. Results and discussion

### 3.1. Is OC preserved with tephra in the marine sediments?

All tephra layers analyzed in this study contained OC (Fig. 1), with tephra layers at U1396C containing an average of 0.13 ± 0.08 wt%, U1339D 0.55 ± 1.19 wt% and 553 A/555 containing 0.49 ± 0.51 wt% OC (all 11 ± SD) (Supplementary Data 1). Freshly created tephra erupted from the volcano is devoid of OC, hence, the OC within tephra layers is either (a) allochthonous due to physical admixture between adjacent OC-free tephra and OC-bearing biogenic sediments, or (b) the scavenging of OC to settling tephra particles in the water column or (c) is autochthonous and related to microbial generation of OC in situ.

The samples were taken from the interior of the tephra layers beyond the visually identifiable zone of bioturbation, if indeed such zones were present at all. Considerable care was also taken during sampling of the cores to avoid cross-contamination during handling. The greatest relative difference between the average OC concentration of the tephra layers (0.5 wt%) and that of the background sediment (1.1 wt%) occurs at site U1339D. Thus, background sediments would have to comprise >50% of the tephra layers at this site to generate the observed levels of OC if they were solely derived from mixing in of background sediment. At the Montserrat and North Atlantic sites, the relative contribution of background sediments would have to be considerably higher than 50%, and we have no evidence to support such a process. It is possible for airfall tephra to be distinguished from reworked tephra and so where possible we complete a visual assessment of this (Hopkins et al., 2020), confirming the majority of tephras indeed have characteristics of primary airfall. For the tephras from Site U1339, this assessment has been done in previous work, indicating the colour and contacts (sharp basal, gradational upper) are representative of airfall tephra (Longman et al., 2021b, Supplementary Fig. 3). For Site U1396C, we selected a sample of the studied tephras and in all cases identify similar features (Supplementary Fig. 4). We performed a similar assessment on the Site 553 A tephras, and find it also appears to be airfall-derived, with little evidence of reworking (Supplementary Fig. 5).

Another alternative is scavenging of OC on sinking tephra particles, although little is known about the scale of this process, and so we assume it is not as significant as local production. We would assume that OC scavenged to tephra particles has a carbon isotopic composition close to particulate organic carbon (around −22‰; (Peterson and Fry, 1987). As all tephra layers other than a small number at U1339 have δ13C values > − 24‰ (Fig. 2), we believe scavenging is not a major source of OC to these environments. We therefore suggest most of the OC preserved in the tephra layers is autochthonous and derived from in situ microbial activity, but with the caveat that OC scavenged by sinking tephra grains is also a potential source.

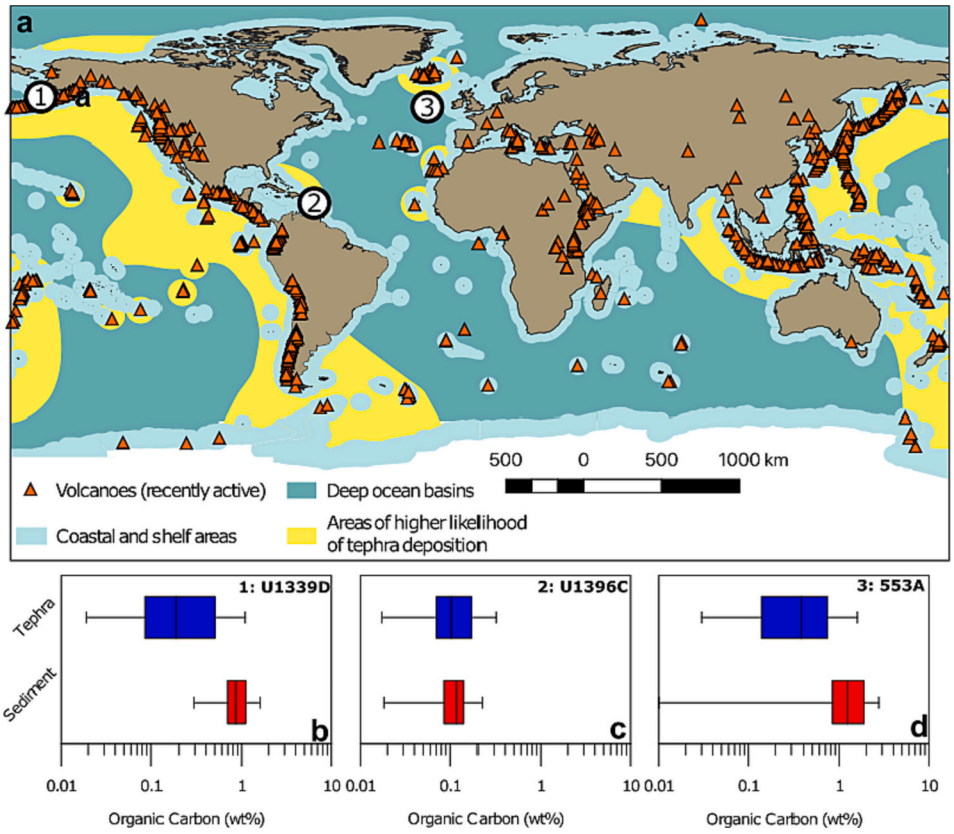


**Fig. 1.** Organic carbon content in tephra and sediments from study sites. (a) Global map indicating location of three study sites 1) U1339D Bering Sea, 2) U1396C Montserrat and 3) 553 A North Atlantic. Also indicated are locations of volcanoes, and regions of the ocean in which tephra deposition is likely. Figure adapted from (Longman et al., 2020). (b-d) Box and whisker diagrams of data. (b) Bering Sea (U1339D), (c) offshore Montserrat (U1396C), (d) North Atlantic (553 A and 555). Boxes are defined between the first and third quartile (interquartile range; IQR), with minimum and maximum whiskers representative of 1.5 times the IQR, and with outliers (>1.5 times IQR) removed.

### 3.2. What mechanisms lead to this OC preservation?

The retention of OC in tephra-rich sediments is likely a feature of the geochemical composition of the tephra. The two main mechanisms by which tephra can enhance OC preservation in marine sediments are by reducing OC exposure to dissolved $O_2$ in porewaters and by formation of OC-reactive metal complexes (Longman et al., 2019). Porewater profiles of dissolved Mn and Fe at Site U1396 suggest that low to zero oxygen conditions prevail throughout most of the ~130 m length of the core (Longman et al., 2023; Murray et al., 2018). SEM images reveal the presence of framboidal pyrite within vesicles in glass fragments of a tephra layer (Fig. 3). This observation requires the existence of anoxic microenvironments within the tephra layer because porewater dissolved $SO_4^{2-}$ concentrations are close to oxic open ocean levels throughout the depth of Site U1396 (Murray et al., 2018), and pyrite was not observed in any background sediment samples. The anoxic conditions required to form the pyrite likely arose because of oxidation of silicate bound $Fe^{II}$ in the tephra by a coupled electron transfer reaction (Hembury et al., 2012). The tephra layer illustrated in Fig. 3 is from a sub-seafloor depth of ~80 m (corresponding to an age of 2.36 Ma (Fraass et al., 2017; Palmer et al., 2016), and pyrite framboids are commonly well-preserved in the geologic record (Wilkin et al., 1996); hence they could have formed at any point since tephra deposition.

Globally, ~20% of marine OC is preserved via complexation with reactive iron ($Fe_R$) phases (Barber et al., 2017; Lalonde et al., 2012; Longman et al., 2022). Within the Bering Sea samples analyzed here, the fraction of OC associated with reactive Fe (fOC—$Fe_R$) in the background sediment (average 31 ± 15%, 1SD, $n$ = 23) is similar to the global average, but within the tephra layers, fOC-$Fe_R$ increases to an average of 79 ± 13% (1SD, $n$ = 14; Longman et al., 2021b). Similar trends are observed in Holes 553 A and 555, where fOC-$Fe_R$ values are on average 63 ± 15% (1 SD, $n$ = 7) for tephra, and 30 ± 6% (1 SD, n = 23) for background sediment (Supplementary Data 2, Fig. 2). These results indicate that even in layers that do not consist purely of tephra, fOC-Fe values are higher than 20%. This observation suggests that dispersed ash, proposed to comprise a volumetrically greater amount of ash in marine sediments than discrete layers in the Pacific Ocean (Scudder et al., 2016; Scudder et al., 2014) and in the Caribbean (Longman et al., 2023) may also provide FeR to protect OC.

By comparison, the highest fOC-$Fe_R$ observed in marine sediments elsewhere is ~40% on the deltaic Washington coast of North America and ~ 30% in sediments underlying the equatorial Pacific upwelling zone (Lalonde et al., 2012), although occasional outliers may be higher than these averages. Even in soils, fOC-$Fe_R$ values are generally not above 30% (Chen et al., 2020; Longman et al., 2022; Zhao et al., 2016), demonstrating the uniqueness of tephra-rich sediments in this respect. The increased $Fe_R$-OC complexation within the tephra layers may be linked to the high proportion of $Fe^{II}$ within tephra deposits (Homoky et al., 2011), which stabilises OC via inner-sphere complexation (Barber et al., 2017).

The oldest sediments analyzed from U1339D are in section 21H4 and were deposited between 700 and 745 kyr ago (Takahashi et al., 2011), whilst those at Hole 553 A are likely ~56 million years old (Backman, 1984; Longman et al., 2021a). These data thus document the oldest known example of a strong linkage between OC and FeR, and are an order of magnitude older than those reported previously (Faust et al., 2021; Longman et al., 2021b). Thus, FeR-OC coupling may serve as a mechanism for the long-term burial of OC, potentially providing the

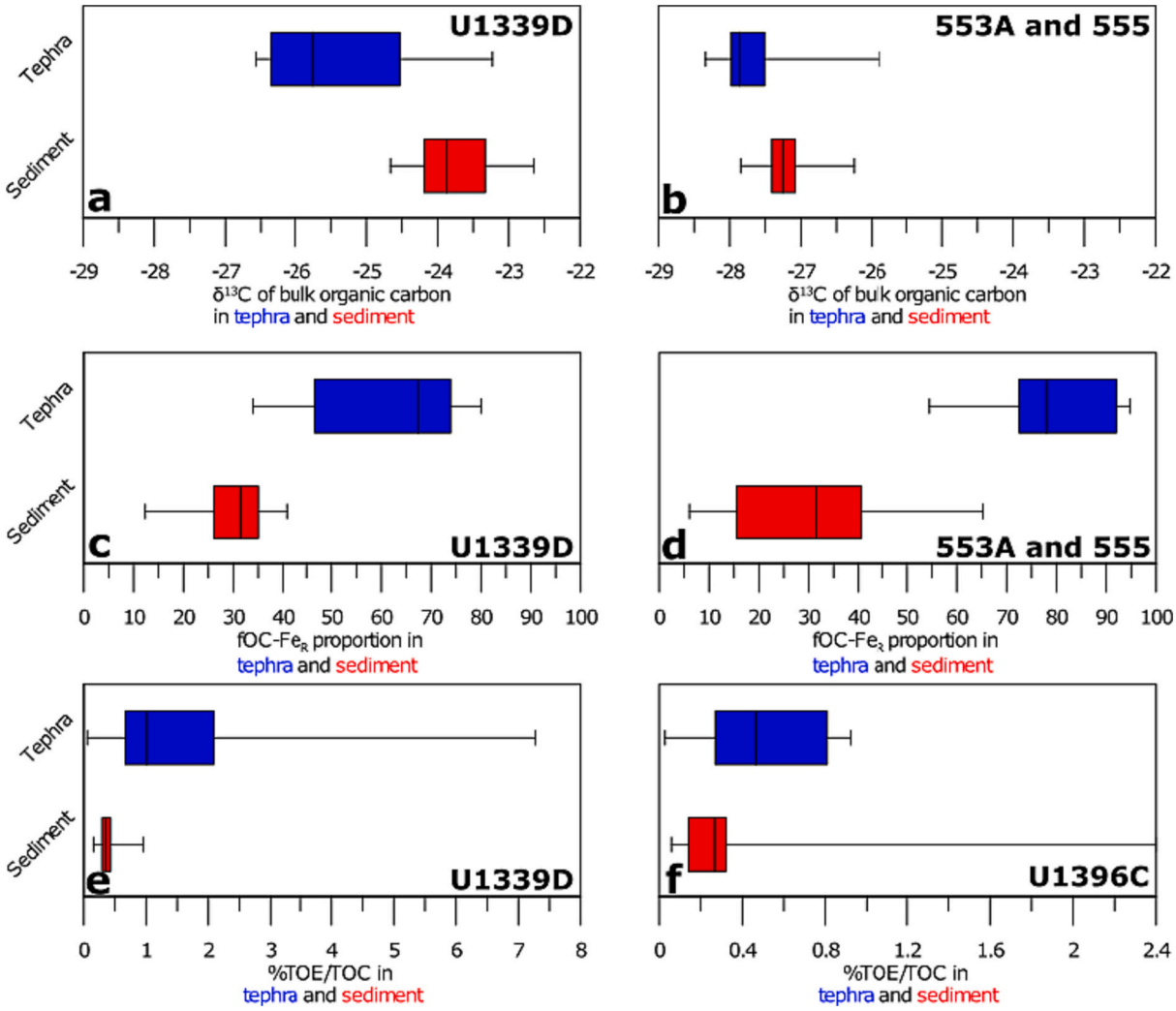


**Fig. 2.** Bulk carbon isotope composition and proportion of organic carbon associated with reactive iron of samples. (a) Carbon isotope data from the Bering Sea (U1339D) and (b) the North Atlantic (Holes 553 A and 555). (c) the fraction of organic carbon associated with reactive iron (fOC-$Fe_R$) for the Bering Sea and North Atlantic (d). The TOE/TOC ratio is presented for the Bering Sea (e) and Montserrat (f). Boxes are defined between the first and third quartile (interquartile range; IQR), with minimum and maximum whiskers representative of 1.5 times the IQR, and with outliers (>1.5 times IQR) removed.

means by which otherwise labile OC may be preserved in marine sediments (Hemingway et al., 2019).

### 3.3. What kind of OC is being preserved in tephra layers?

The data presented above clearly suggest that a significant proportion of the OC found within and adjacent to tephra layers is preserved as a direct result of deposition of the tephra. However, the composition and source of this OC remains unclear. Nevertheless, the data indicate that the tephra-associated OC is different in composition from OC in non-tephra bearing sediments. In Montserrat, extractable organic carbon efficiencies (as measured by total organic extract/total OC (TOE/TOC; Supplementary Data 3) are higher for the tephra-rich sediments (<10 wt % $CaCO_3$, TOE/TOC = 0.80 ± 0.17%; 1SD; $n$ = 18) than for the tephra-poor sediments (>10 wt% $CaCO_3$, TOE/TOC = 0.23 ± 0.02%; 1SD; $n$ = 45). In the Bering Sea, tephra samples show similarly high TOE/TOC ratios (TOE/TOC = 1.53 ± 0.32%; 1SD; $n$ = 23) compared to the sediments (TOE/TOC = 0.39 ± 0.02%; 1SD; n = 45). These data indicate that the OC within the tephra-rich sediments in both locations is more labile (lipid-rich and extractable into organic solvent, TOE) than OC in the background hemipelagic sediments.

Bulk carbon isotope analyses of the OC also reveal differences between the tephras and sediments, with a shift toward more negative $\delta^{13}C$ values for tephra-hosted OC in samples from both the Bering Sea and the North Atlantic (Fig. 2). In the Bering Sea, the tephras are depleted in $^{13}C$ ($\delta^{13}C = -25.7 \pm 0.3$ ‰; 1SE, $n$ = 14) compared to background sediments ($\delta^{13}C = -23.8 \pm 0.1$ ‰; 1SE, n = 23). A smaller offset in $\delta^{13}C$ values is seen in the North Atlantic data (Supplementary Data 2), with only slightly more negative $\delta^{13}C$ values for the tephras ($\delta^{13}C = -27.8 \pm 0.1$ ‰; 1SE, $n$ = 31) than the sediments ($\delta^{13}C = -27.2 \pm 0.03$ ‰; 1SE, $n$ = 88), but the difference between the tephra and sediment $\delta^{13}C$ values is smaller than that observed in the Bering Sea samples. In these cores, a greater overall depletion of the $\delta^{13}C$ signature may result from microbial decomposition and diagenetic turnover; processes that can affect the carbon isotopic mixture over thousands to millions of years (Blumenberg et al., 2015; Shah Walter et al., 2018). As with the bulk $\delta^{13}C$, the carbon isotope composition of OC associated with reactive Fe ($\delta^{13}C_{Fe\text{-}OC}$) of the tephra layers in the Bering Sea is also consistently, although not statistically significantly, more negative than in the sediments, with an average of −25.4 ± 1 ‰ (1SE, $n$ = 22) in tephra and − 23.9 ± 1 ‰ (1SE, $n$ = 44) in sediments (Longman et al., 2021b).

There are no major rivers feeding the sampling locations (Fig. 1), so terrestrial contributions of OC are unlikely at any of the locations. The typical carbon isotopic signature of marine OC is usually on the order of about −22‰ (Peterson and Fry, 1987). Hence the tephra layers contain $^{13}C$ depleted OC (Fig. 2). Variations in the levels of remineralization are

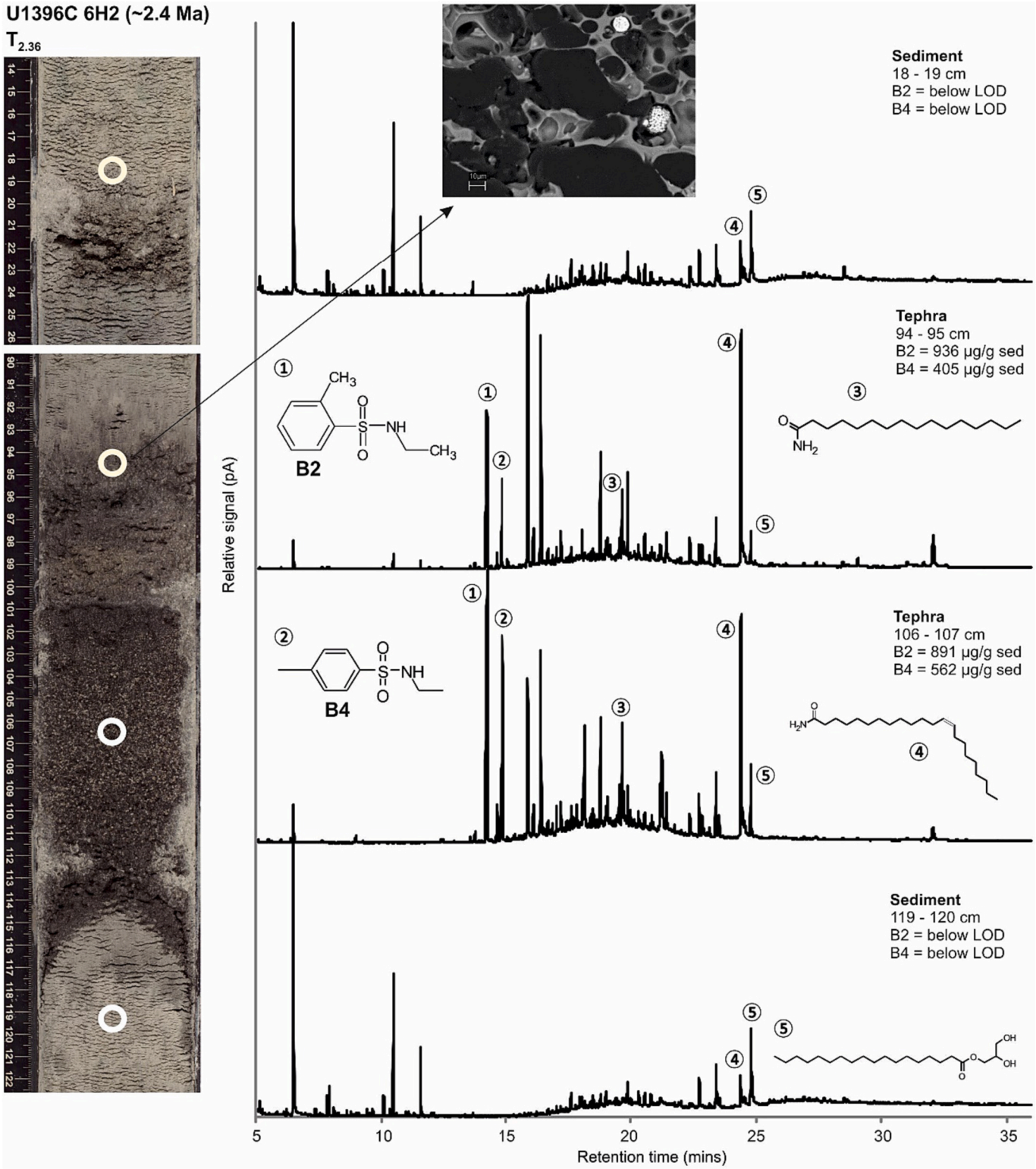


**Fig. 3.** GC–MS total ion chromatograms of total organic extracts of sub-core 6H2 from Montserrat (U1396C). Circles on the core photograph indicate the sample locations for tephra-rich (<10% $CaCO_3$) and background sediments (>10% $CaCO_3$). Total ion chromatograms are scaled to the maximum peak height in each case for comparison and are typical of all those tephra-rich and background sediments examined throughout U1396C (sediment $n = 53$, visible tephra $n = 10$). Peak identifications are: 1 = n-ethyl-2-methylbenzene-1-sulfonamide; 2 = n-ethyl-4-methylbenzene-1-sulfonamide; 3 = hexadecanamide; 4 = 13-docosenamide; 5 = 2,3-dihydroxypropyl octadecenoate.

unlikely to have modified the isotopic composition of the organic matter of the sediment (Hedges et al., 1999). Fatty acids could represent such a source, as lipid compounds are depleted in $^{13}C$ relative to bulk sediment biomass, with microbial fatty acid $\delta^{13}C$ values ranging from −30 to −45 ‰, depending on the carbon source (Gong and Hollander, 1997; Hayes, 2001).

GC–MS analyses of lipid extracts from the Montserrat samples reveal that the lipid composition of the hemipelagic sediments containing no visible tephra ($n = 53$) is typical of such sediments (i.e., they exhibit a homologous series of alkanes, acids, alcohols and mono- and diglycerides). In contrast, the horizons containing visible tephra ($n = 10$) consistently display markedly different compositions, as revealed in the GC–MS total ion chromatograms (Fig. 3). Chromatograms from the Montserrat tephra samples are dominated by a small number of compounds, notably a pair of benzenosulfonamides, the fatty acid amides hexadecanimide and 13-docosenamide, and 2,3-dihydroxypropyl octadecenoate (the peak identification protocol is described in the Methods section), compounds that are either not detectable at all or are present in very low relative concentrations in background sediments (Fig. 3, Supplementary Data 4).

Benzenosulfonamides are widely used as plasticisers (Strong et al., 1991) and the IODP and ODP cores are collected and stored in plastic liners. Hence, such a source must be considered when evaluating the presence of these compounds in the tephra layers. GC–MS analyses were undertaken of all the plastic material that could potentially have encountered the samples (Supplementary Fig. 2): no benzenosulfonamides were identified in any of these materials. Further, the sediment samples were prepared in the same manner as the tephra samples, but critically, benzenosulfonamides were not identified in any of the sediments. Hence, while we cannot definitively dispel the notion of an anthropogenic origin for these compounds, we find no evidence to support any other conclusion than that they were produced in situ in the tephra.

Hexadecanimide, 13-docosemanide (although also used as a slip additive in plastic oil production) and 2,3-dihydroxypropyl octadecenoate have all previously been identified as bacterial metabolites (Mićić et al., 2011; Scherf and Rullkötter, 2009), and hexadecanimide is a ubiquitous secondary metabolite in microbial communities (Scherf and Rullkötter, 2009). Hence, the presence of these compounds within the tephra layer is compatible with an autochthonous origin for the OC. In contrast, the evidence for a primary marine biogenic origin of the sulfonamides is less clear. The only reported natural product sulfonamide from the marine environment is from the sponge *Pseudoceratina purpurea* (Mujumdar et al., 2016; Mujumdar and Poulsen, 2015). However, laboratory studies have identified the production of sulfonamides from *Streptomyces* species (Baunach et al., 2015; Hu et al., 2019). *Streptomyces* are amongst the most widespread strains of bacteria within the marine environment and are known to produce a wide range of complex heterocyclic natural products (Dharmaraj, 2010). Unfortunately, none of the samples considered in this study were collected under conditions that permitted analyses of their microbiological communities. The possibility that sulfonamides are produced within the tephra layers by microbial activity, is worthy of further investigation.

Support for the presence of microbial communities within the tephra layers comes from studies that found that the addition of tephra to surface seawater stimulated the growth of autotrophic and heterotrophic microorganisms (Zhang et al., 2017). A new bacterial genus and species (*Thiolava veneris*) was discovered around the summit of the Canary Archipelago, and this organism used the volcanic substrate as an energy source (Danovaro et al., 2017). Distinct microbial communities have also been recorded in tephra deposits at the sediment-water interface from a subglacial volcanic caldera in Iceland (Gaidos et al., 2004), in ~100 kyr marine sediments NE of Japan (Inagaki et al., 2003), and in marine tephra deposits close to the sediment-water interface from the Yap trench in the western Pacific Ocean (Li et al., 2020). In addition, it has long been recognised that Fe-oxidising bacteria inhabit the glassy margins of ocean floor basalts (Furnes et al., 2002; Thorseth et al., 2001). Further, laboratory evidence indicates the formation of cyanobacterial mats colonising bare tephra surfaces within 2 months of deposition (Fiantis et al., 2016).

In summary, the differences between the $\delta^{13}C$ of the tephra and sediment OC (both reactive-Fe bound and bulk) in the Bering Sea and in the North Atlantic suggests that a different type of OC is present in the tephra, and that this difference is preserved in deeply buried sediments. This conclusion is supported by the organic geochemistry, which demonstrates a clear difference in the nature of the OC preserved in tephra layers compared to that present in the background marine sediments. Thus, there are active microbial communities in tephra layers buried over 100 m below the seafloor, and that have been isolated from direct seawater contact for over 4 Myr (and even 56 Myr in the case of the North Atlantic tephra). Alternatively, the tephra provides an environment that leads to enhanced preservation of labile organic compounds. Water-tephra interactions have occurred on Earth throughout its history and have been documented on Mars within the last 10 million years (Cousins and Crawford, 2011). If the OC found in the tephra layers do represent markers for microbial activity, this observation suggests that areas of water-volcano interaction represent a potential site for discovering evidence of current or past microbial activity on Mars, hence these areas could be fruitful targets in the search for Martian evidence of lifeforms in future expeditions.

## 4. Conclusions

Tephra layers buried to depths of up to ~130 m below seafloor, within marine sediments and spanning ages of up to ~56 Ma, exhibit significantly higher concentrations of organic carbon (OC) than would be expected from simple admixture with surrounding background sediments. The $\delta^{13}C$ and molecular composition of OC within the tephra layers are also distinct from the surrounding sediments. These observations are most compatible with in situ production of OC within the tephra by a distinct microbiological community. Preservation of OC within the tephra layers is enhanced by the generation of anoxic microenvironments, and by complexation of the OC by reactive Fe generated by the tephra. These observations suggest that ancient tephra layers may be valuable archives of microbial activity.

## Data availability

All data are uploaded as supplementary data sets.

## Acknowledgements

Funding for this research was provided by NERC grant NE/K00543X/1 to Gernon and Palmer and the US National Science Foundation under grant numbers 1360077 and 1715106 to McManus. We are indebted to A. Tonkin for providing knowledge and experience in CHN analysis at Plymouth University, UK and A. Hartwell at the University of Akron, USA for assistance with the reactive metal analyses. We also thank the staff at the IODP core repository Bremen, the IODP Kochi Core Centre (KCC) Japan, and the IODP Gulf Coast Core Repository (GCR) at Texas A&M University, for assistance with sampling. We are grateful for input of the reviewers, whose comments helpe dus to improve the paper.

## Appendix A. Supplementary data

Supplementary data to this article can be found online at https://doi.org/10.1016/j.marchem.2023.104334.

## References


Backman, J., 1984. Cenozoic calcareous nannofossil biostratigraphy from the north-eastern Atlantic Ocean-Deep Sea drilling project leg 81. Initial Rep. Deep Sea Drill. Proj. 81, 403–428.

Backman, J., Morton, A.C., Roberts, D.G., Brown, S., Krumsiek, K., 1984. Geochronology of the Lower Eocene and Upper Paleocene Sequences of Leg 81. Initial Reports DSDP, Leg 81, Southampton to Azores, pp. 877–882.

Barber, A., Brandes, J., Leri, A., Lalonde, K., Balind, K., Wirick, S., Wang, J., Gélinas, Y., 2017. Preservation of organic matter in marine sediments by inner-sphere interactions with reactive iron. Sci. Rep. 7, 366. https://doi.org/10.1038/s41598-017-00494-0.

Baunach, M., Ding, L., Willing, K., Hertweck, C., 2015. Bacterial synthesis of unusual sulfonamide and sulfone antibiotics by Flavoenzyme-mediated sulfur dioxide capture. Angew. Chem. Int. Ed. 54, 13279–13283. https://doi.org/10.1002/anie.201506541.

Blumenberg, M., Thiel, V., Reitner, J., 2015. Organic matter preservation in the carbonate matrix of a recent microbial mat - is there a "mat seal effect"? Org. Geochem. 87, 25–34. https://doi.org/10.1016/j.orggeochem.2015.07.005.

Browning, T.J., Bouman, H.A., Henderson, G.M., Mather, T.A., Pyle, D.M., Schlosser, C., Woodward, E.M.S., Moore, C.M., 2014. Strong responses of Southern Ocean phytoplankton communities to volcanic ash. Geophys. Res. Lett. 41, 2851–2857. https://doi.org/10.1002/2014GL059364.

Chen, C., Hall, S.J., Coward, E., Thompson, A., 2020. Iron-mediated organic matter decomposition in humid soils can counteract protection. Nat. Commun. 11 (1), 1–13. https://doi.org/10.1038/s41467-020-16071-5.

Cousins, C.R., Crawford, I.A., 2011. Volcano-ice interaction as a microbial habitat on earth and mars. Astrobiology. https://doi.org/10.1089/ast.2010.0550.

Danovaro, R., Canals, M., Tangherlini, M., Dell'Anno, A., Gambi, C., Lastras, G., Amblas, D., Sanchez-Vidal, A., Frigola, J., Calafat, A.M., Pedrosa-Pàmies, R., Rivera, J., Rayo, X., Corinaldesi, C., 2017. A submarine volcanic eruption leads to a novel microbial habitat. Nat. Ecol. Evol. 1, 144. https://doi.org/10.1038/s41559-017-0144.

Dharmaraj, S., 2010. Marine Streptomyces as a novel source of bioactive substances. World J. Microbiol. Biotechnol. 26, 2123–2139. https://doi.org/10.1007/s11274-010-0415-6.

Faust, J.C., Tessin, A., Fisher, B.J., Zindorf, M., Papadaki, S., Hendry, K.R., Doyle, K.A., März, C., 2021. Millennial scale persistence of organic carbon bound to iron in Arctic marine sediments. Nat. Commun. 12, 1–9. https://doi.org/10.1038/s41467-020-20550-0.

Fiantis, D., Nelson, M., Shamshuddin, J., Goh, T.B., Van Ranst, E., 2016. Initial carbon storage in new tephra layers of Mt. Talang in Sumatra as affected by Pioneer plants. Commun. Soil Sci. Plant Anal. 47, 1792–1812. https://doi.org/10.1080/00103624.2016.1208755.

Fisher, B.J., Moore, O.W., Faust, J.C., Peacock, C.L., März, C., 2020. Experimental evaluation of the extractability of iron bound organic carbon in sediments as a function of carboxyl content. Chem. Geol. 556, 119853 https://doi.org/10.1016/j.chemgeo.2020.119853.

Fraass, A.J., Palmer, M., Martinez-Colon, M., Jutzeler, M., Aljahdali, M., Ishizuka, O., Le Friant, A.L.F., Burns, S.J., Hatfield, R.G., Leckie, R.M., Wall-Palmer, D.W.-P., Talling, P.J., 2017. A revised Plio-Pleistocene age model and paleoceanography of the northeastern Caribbean Sea: IODP site U1396 off Montserrat, Lesser Antilles. Stratigraphy 13, 183–203. https://doi.org/10.29041/strat.13.3.183-203.

Furnes, H., Thorseth, I.H., Torsvik, T., Muehlenbachs, K., Staudigel, H., Tumyr, O., 2002. Identifying bio-interaction with basaltic glass in oceanic crust and implications for estimating the depth of the oceanic biosphere: a review. Geol. Soc. Spec. Publ. 202, 407–421. https://doi.org/10.1144/GSL.SP.2002.202.01.21.

Gaidos, E., Lanoil, B., Thorsteinsson, T., Graham, A., Skidmore, M., Han, S.K., Rust, T., Popp, B., 2004. A viable microbial community in a subglacial volcanic crater lake, Iceland. Astrobiology 4, 327–344. https://doi.org/10.1089/ast.2004.4.327.

Gong, C., Hollander, D.J., 1997. Differential contribution of bacteria to sedimentary organic matter in oxic and anoxic environments, Santa Monica Basin, California. In: Organic Geochemistry. Pergamon, pp. 545–563. https://doi.org/10.1016/S0146-6380(97)00018-1.

Goñi, M.A., Teixeira, M.J., Perkeya, D.W., 2003. Sources and distribution of organic matter in a river-dominated estuary (Winyah Bay, SC, USA). Estuar. Coast. Shelf Sci. 57, 1023–1048. https://doi.org/10.1016/S0272-7714(03)00008-8.

Hayes, J.M., 2001. Fractionation of carbon and hydrogen isotopes in biosynthetic processes. Rev. Mineral. Geochem. 43, 191–277. https://doi.org/10.2138/gsrmg.43.1.225.

Hedges, J.I., Hu, F.S., Devol, A.H., Hartnett, H.E., Tsamakis, E., Keil, R.G., 1999. Sedimentary organic matter preservation; a test for selective degradation under oxic conditions. Am. J. Sci. 299, 529–555. https://doi.org/10.2475/ajs.299.7-9.529.

Hembury, D.J., Palmer, M.R., Fones, G.R., Mills, R.A., Marsh, R., Jones, M.T., 2012. Uptake of dissolved oxygen during marine diagenesis of fresh volcanic material. Geochim. Cosmochim. Acta 84, 353–368. https://doi.org/10.1016/J.GCA.2012.01.017.

Hemingway, J.D., Rothman, D.H., Grant, K.E., Rosengard, S.Z., Eglinton, T.I., Derry, L.A., Galy, V.V., 2019. Mineral protection regulates long-term global preservation of natural organic carbon. Nature 570, 228–231. https://doi.org/10.1038/s41586-019-1280-6.

Hess, S., Kuhnt, W., 1996. Deep-sea benthic foraminiferal recolonization of the 1991 Mt. Pinatubo ash layer in the South China Sea. Mar. Micropaleontol. 28, 171–197. https://doi.org/10.1016/0377-8398(95)00080-1.

Hess, S., Kuhnt, W., Hill, S., Kaminski, M.A., Holbourn, A., de Leon, M., 2001. Monitoring the recolonization of the Mt Pinatubo 1991 ash layer by benthic foraminifera. Mar. Micropaleontol. 43, 119–142. https://doi.org/10.1016/S0377-8398(01)00025-1.

Homoky, W.B., Hembury, D.J., Hepburn, L.E., Mills, R.A., Statham, P.J., Fones, G.R., Palmer, M.R., 2011. Iron and manganese diagenesis in deep sea volcanogenic sediments and the origins of pore water colloids. Geochim. Cosmochim. Acta 75, 5032–5048. https://doi.org/10.1016/J.GCA.2011.06.019.

Hopkins, J.L., Wysoczanski, R.J., Orpin, A.R., Howarth, J.D., Strachan, L.J., Lunenburg, R., McKeown, M., Ganguly, A., Twort, E., Camp, S., 2020. Deposition and preservation of tephra in marine sediments at the active Hikurangi subduction margin. Quat. Sci. Rev. 247, 106500 https://doi.org/10.1016/j.quascirev.2020.106500.

Hu, Z., Awakawa, T., Ma, Z., Abe, I., 2019. Aminoacyl sulfonamide assembly in SB-203208 biosynthesis. Nat. Commun. 10 https://doi.org/10.1038/s41467-018-08093-x.

Inagaki, F., Suzuki, M., Takai, K., Oida, H., Sakamoto, T., Aoki, K., Nealson, K.H., Horikoshi, K., 2003. Microbial communities associated with geological horizons in coastal subseafloor sediments from the Sea of Okhotsk. Appl. Environ. Microbiol. 69, 7224–7235. https://doi.org/10.1128/AEM.69.12.7224-7235.2003.

Kostka, J.E., Luther, G.W., 1994. Partitioning and speciation of solid phase iron in saltmarsh sediments. Geochim. Cosmochim. Acta 58, 1701–1710. https://doi.org/10.1016/0016-7037(94)90531-2.

Lalonde, K., Mucci, A., Ouellet, A., Gélinas, Y., 2012. Preservation of organic matter in sediments promoted by iron. Nature 483, 198–200. https://doi.org/10.1038/nature10855.

Langmann, B., Zakšek, K., Hort, M., Duggen, S., 2010. Volcanic ash as fertiliser for the surface ocean. Atmos. Chem. Phys. 10, 3891–3899. https://doi.org/10.5194/acp-10-3891-2010.

Le Friant, A., Ishizuka, O., Stroncik, N.A., Expedition 340 Scientists, T, 2013. Proc. IODP, 340. Integrated Ocean Drilling Program Management International, Inc., Tokyo..

Lee, C.-T.A., Jiang, H., Ronay, E., Minisini, D., Stiles, J., Neal, M., 2018. Volcanic ash as a driver of enhanced organic carbon burial in the cretaceous. Sci. Rep. 8, 4197. https://doi.org/10.1038/s41598-018-22576-3.

Li, L., Bai, S., Li, J., Wang, S., Tang, L., Dasgupta, S., Tang, Y., Peng, X., 2020. Volcanic ash inputs enhance the deep-sea seabed metal-biogeochemical cycle: a case study in the yap trench, western Pacific Ocean. Mar. Geol. 430, 106340 https://doi.org/10.1016/j.margeo.2020.106340.

Li, T., Li, J., Longman, J., Zhang, Z.-X., Qu, Y., Chen, S., Bai, S., Dasgupta, S., Xu, H., Ta, K., Liu, S., 2023. Chemolithotrophic biosynthesis of organic carbon associated with volcanic ash in the Mariana trough, Pacific Ocean. Communicat. Earth & Environ. 4.

Longman, J., Palmer, M.R., Gernon, T.M., Manners, H.R., 2019. The role of tephra in enhancing organic carbon preservation in marine sediments. Earth Sci. Rev. 192, 480–490. https://doi.org/10.1016/j.earscirev.2019.03.018.

Longman, J., Palmer, M.R., Gernon, T.M., 2020. Viability of greenhouse gas removal via artificial addition of volcanic ash to the ocean. Anthropocene 32. https://doi.org/10.1016/j.ancene.2020.100264.

Longman, J., Gernon, T.M., Palmer, M.R., Jones, M.T., Stokke, E.W., Svensen, H.H., 2021a. Marine diagenesis of tephra aided the Paleocene-Eocene thermal maximum termination. Earth Planet. Sci. Lett. 571, 117101.

Longman, J., Gernon, T.M., Palmer, M.R., Manners, H.R., 2021b. Tephra deposition and bonding with reactive oxides enhances burial of organic carbon in the Bering Sea. Glob. Biogeochem. Cycles 35. https://doi.org/10.1029/2021GB007140 e2021GB007140.

Longman, J., Mills, B.J.W., Manners, H.R., Gernon, T.M., Palmer, M.R., 2021c. Late Ordovician climate change and extinctions driven by elevated volcanic nutrient supply. Nat. Geosci. 14, 924–929. https://doi.org/10.1038/s41561-021-00855-5.

Longman, J., Faust, J.C., Bryce, C., Homoky, W.B., März, C., 2022. Organic carbon burial with reactive Iron across global environments. Glob. Biogeochem. Cycles 36. https://doi.org/10.1029/2022GB007447 e2022GB007447.

Longman, J., Dunlea, A.G., Böning, P., Palmer, M.R., Gernon, T.M., McManus, J., Manners, H.R., Homoky, W.B., Pahnke, K., 2023. Release of tephra-hosted iron during early diagenesis fingerprinted by iron isotopes. Earth Planet. Sci. Lett. 605, 118016 https://doi.org/10.1016/J.EPSL.2023.118016.

Lowe, D.J., 2011. Tephrochronology and its application: a review. Quat. Geochronol. 6, 107–153. https://doi.org/10.1016/J.QUAGEO.2010.08.003.

Luo, M., Torres, M.E., Hong, W.L., Pape, T., Fronzek, J., Kutterolf, S., Mountjoy, J.J., Orpin, A., Henkel, S., Huhn, K., Chen, D., Kasten, S., 2020. Impact of iron release by volcanic ash alteration on carbon cycling in sediments of the northern Hikurangi margin. Earth Planet. Sci. Lett. 541, 116288 https://doi.org/10.1016/j.epsl.2020.116288.

Luo, M., Hong, W.-L., Torres, M.E., Kutterolf, S., Pank, K., Hopkins, J.L., Solomon, E.A., Wang, K.-L., Lee, H.-Y., 2023. Volcanogenic aluminosilicate alteration drives formation of authigenic phases at the northern Hikurangi margin: implications for subseafloor geochemical cycles. Chem. Geol. 619, 121317 https://doi.org/10.1016/j.chemgeo.2023.121317.

Mićić, V., Kruge, M.A., Köster, J., Hofmann, T., 2011. Natural, anthropogenic and fossil organic matter in river sediments and suspended particulate matter: a multi-molecular marker approach. Sci. Total Environ. 409, 905–919. https://doi.org/10.1016/j.scitotenv.2010.11.009.

Mujumdar, P., Poulsen, S.A., 2015. Natural product primary sulfonamides and primary Sulfamates. J. Nat. Prod. 78, 1470–1477. https://doi.org/10.1021/np501015m.

Mujumdar, P., Teruya, K., Tonissen, K.F., Vullo, D., Supuran, C.T., Peat, T.S., Poulsen, S. A., 2016. An unusual natural product primary sulfonamide: synthesis, carbonic anhydrase inhibition, and protein X-ray structures of Psammaplin C. J. Med. Chem. 59, 5462–5470. https://doi.org/10.1021/acs.jmedchem.6b00443.

Murray, N.A., Muratli, J.M., Hartwell, A.M., Manners, H., Megowan, M.R., Goñi, M., Palmer, M., McManus, J., 2016. Data report: dissolved minor element compositions, sediment major and minor element concentrations, and reactive iron and manganese data from the Lesser Antilles volcanic arc region. In: IODP Expedition 340 Sites U1394, U1395, U1396, U1399, and U1400. Proceedings of the Integrated Ocean Drilling Program, 340. https://doi.org/10.2204/iodp.proc.340.207.2016.

Murray, N.A., McManus, J., Palmer, M.R., Haley, B., Manners, H., 2018. Diagenesis in tephra-rich sediments from the Lesser Antilles volcanic arc: pore fluid constraints. Geochim. Cosmochim. Acta 228, 119–135. https://doi.org/10.1016/J.GCA.2018.02.039.

Olgun, N., Duggen, S., Croot, P.L., Delmelle, P., Dietze, H., Schacht, U., Óskarsson, N., Siebe, C., Auer, A., Garbe-Schönberg, D., 2011. Surface Ocean iron fertilization: the role of airborne volcanic ash from subduction zone and hot spot volcanoes and related iron fluxes into the Pacific Ocean. Glob. Biogeochem. Cycles 25, n/a–n/a. https://doi.org/10.1029/2009GB003761.

Pabortsava, K., Lampitt, R.S., Benson, J., Crowe, C., McLachlan, R., Le Moigne, F.A.C., Mark Moore, C., Pebody, C., Provost, P., Rees, A.P., Tilstone, G.H., Woodward, E.M. S., 2017. Carbon sequestration in the deep Atlantic enhanced by Saharan dust. Nat. Geosci. 10, 189–194. https://doi.org/10.1038/ngeo2899.

Palmer, M.R., Hatter, S.J., Gernon, T.M., Taylor, R.N., Cassidy, M., Johnson, P., Le Friant, A., Ishizuka, O., 2016. Discovery of a large 2.4 Ma Plinian eruption of Basse-Terre, Guadeloupe, from the marine sediment record. Geology 44, 123–126. https://doi.org/10.1130/G37193.1.

Peterson, B.J., Fry, B., 1987. Stable isotopes in ecosystem studies. Annu. Rev. Ecol. Syst. 18 18, 293–320. https://doi.org/10.1016/0198-0254(88)92720-3.

Pyle, D.M., 1995. Mass and energy budgets of explosive volcanic eruptions. Geophys. Res. Lett. 22, 563–566. https://doi.org/10.1029/95GL00052.

Roberts, D.G., Morton, A.C., Backman, J., 1984. Late palaeocene-eocene volcanic events in the northern north atlantic ocean. In: Initial Reports of the Deep Sea Drilling Project, pp. 913–923.

Roy, M., McManus, J., Goñi, M.A., Chase, Z., Borgeld, J.C., Wheatcroft, R.A., Muratli, J. M., Megowan, M.R., Mix, A., 2013. Reactive iron and manganese distributions in seabed sediments near small mountainous rivers off Oregon and California (USA). Cont. Shelf Res. 54, 67–79. https://doi.org/10.1016/J.CSR.2012.12.012.

Scherf, A.K., Rullkötter, J., 2009. Biogeochemistry of high salinity microbial mats - part 1: lipid composition of microbial mats across intertidal flats of Abu Dhabi, United Arab Emirates. Org. Geochem. 40, 1018–1028. https://doi.org/10.1016/j.orggeochem.2009.04.002.

Scudder, R.P., Murray, R.W., Schindlbeck, J.C., Kutterolf, S., Hauff, F., McKinley, C.C., 2014. Regional-scale input of dispersed and discrete volcanic ash to the Izu-Bonin and Mariana subduction zones. Geochem. Geophys. Geosyst. 15, 4369–4379. https://doi.org/10.1002/2014GC005561.

Scudder, R.P., Murray, R.W., Schindlbeck, J.C., Kutterolf, S., Hauff, F., Underwood, M.B., Gwizd, S., Lauzon, R., McKinley, C.C., 2016. Geochemical approaches to the quantification of dispersed volcanic ash in marine sediment. Prog. Earth Planet Sci. 3, 1. https://doi.org/10.1186/s40645-015-0077-y.

Shah Walter, S.R., Jaekel, U., Osterholz, H., Fisher, A.T., Huber, J.A., Pearson, A., Dittmar, T., Girguis, P.R., 2018. Microbial decomposition of marine dissolved organic matter in cool oceanic crust. Nat. Geosci. 11, 334–339. https://doi.org/10.1038/s41561-018-0109-5.

Song, B., Buckner, C.T., Hembury, D.J., Mills, R.A., Palmer, M.R., 2014. Impact of volcanic ash on anammox communities in deep sea sediments. Environ. Microbiol. Rep. 6, 159–166. https://doi.org/10.1111/1758-2229.12137.

Straub, S.M., Schmincke, H.U., 1998. Evaluating the tephra input into Pacific Ocean sediments: distribution in space and time. Geol. Rundsch. 87, 461–476. https://doi.org/10.1007/s005310050222.

Strong, M.J., Garruto, R.M., Wolff, A.V., Chou, S.M., Fox, S.D., Yanagihara, R., 1991. N-butyl benzenesulfonamide: a neurotoxic plasticizer inducing a spastic myelopathy in rabbits. Acta Neuropathol. 81, 235–241. https://doi.org/10.1007/BF00305863.

Sutton, P.A., Rowland, S.J., 2012. High temperature gas chromatography–time-of-flight-mass spectrometry (HTGC–ToF-MS) for high-boiling compounds. J. Chromatogr. A 1243, 69–80. https://doi.org/10.1016/J.CHROMA.2012.04.044.

Takahashi, K., Ravelo, A., Alvarez-Zarikian, C., 2011. Proceedings of the Integrated Ocean drilling program: Expedition reports: Bering Sea paleoceanography. In: Integrated Ocean Drilling Program Management International, Inc., for the Integrated Ocean Drilling Program, College Station, Texas, vol. 323.

Thorseth, I.H., Torsvik, T., Torsvik, V., Daae, F.L., Pedersen, R.B., 2001. Diversity of life in ocean floor basalt. Earth Planet. Sci. Lett. 194, 31–37. https://doi.org/10.1016/S0012-821X(01)00537-4.

Torres, M.E., Hong, W.L., Solomon, E.A., Milliken, K., Kim, J.H., Sample, J.C., Teichert, B.M.A., Wallmann, K., 2020. Silicate weathering in anoxic marine sediment as a requirement for authigenic carbonate burial. Earth Sci. Rev. https://doi.org/10.1016/j.earscirev.2019.102960.

Vaughn, D.R., Caissie, B.E., 2017. Effects of sea-level, sea-ice extent, and nutrient availability on primary production at the Umnak plateau, Bering Sea (IODP site U1339) during marine isotope stage (MIS) 5. Palaeogeogr. Palaeoclimatol. Palaeoecol. 485, 283–292. https://doi.org/10.1016/J.PALAEO.2017.06.020.

Wallmann, K., Aloisi, G., Haeckel, M., Tishchenko, P., Pavlova, G., Greinert, J., Kutterolf, S., Eisenhauer, A., 2008. Silicate weathering in anoxic marine sediments. Geochim. Cosmochim. Acta 72, 2895–2918. https://doi.org/10.1016/j.gca.2008.03.026.

Wall-Palmer, D., Jones, M.T., Hart, M.B., Fisher, J.K., Smart, C.W., Hembury, D.J., Palmer, M.R., Fones, G.R., 2011. Explosive volcanism as a cause for mass mortality of pteropods. Mar. Geol. 282, 231–239. https://doi.org/10.1016/J.MARGEO.2011.03.001.

Wall-Palmer, D., Coussens, M., Talling, P.J., Jutzeler, M., Cassidy, M., Marchant, I., Palmer, M.R., Watt, S.F.L., Smart, C.W., Fisher, J.K., Hart, M.B., Fraass, A., Trofimovs, J., Le Friant, A., Ishizuka, O., Adachi, T., Aljahdali, M., Boudon, G., Breitkreuz, C., Endo, D., Fujinawa, A., Hatfield, R., Hornbach, M.J., Kataoka, K., Lafuerza, S., Maeno, F., Manga, M., Martinez-Colon, M., McCanta, M., Morgan, S., Saito, T., Slagle, A.L., Stinton, A.J., Subramanyam, K.S.V., Tamura, Y., Villemant, B., Wang, F., 2014. Late Pleistocene stratigraphy of IODP site U1396 and compiled chronology offshore of south and south West Montserrat, Lesser Antilles. Geochem. Geophys. Geosyst. 15, 3000–3020. https://doi.org/10.1002/2014GC005402.

White, D.C., Davis, W.M., Nickels, J.S., King, J.D., Bobbie, R.J., 1979. Determination of the sedimentary microbial biomass by extractible lipid phosphate. Oecologia 40, 51–62. https://doi.org/10.1007/BF00388810.

Wilkin, R.T., Barnes, H.L., Brantley, S.L., 1996. The size distribution of framboidal pyrite in modern sediments: an indicator of redox conditions. Geochim. Cosmochim. Acta 60, 3897–3912. https://doi.org/10.1016/0016-7037(96)00209-8.

Zhang, R., Jiang, T., Tian, Y., Xie, S., Zhou, L., Li, Q., Jiao, N., 2017. Volcanic ash stimulates growth of marine autotrophic and heterotrophic microorganisms. Geology 45 (G38833), 1. https://doi.org/10.1130/G38833.1.

Zhao, Q., Poulson, S.R., Obrist, D., Sumaila, S., Dynes, J.J., McBeth, J.M., Yang, Y., 2016. Iron-bound organic carbon in forest soils: quantification and characterization. Biogeosciences 13, 4777–4788. https://doi.org/10.5194/BG-13-4777-2016.